Compact Millimeter and Submillimeter-Wave Photonic Radiometer for Cubesats

Michał Wasiak[1], Gabriel Santamaría Botello[1], Kerlos Atia Abdalmalak[1], Florian Sedlmeir[2], Alfredo Rueda[2,3,4,5,6], Daniel Segovia-Vargas[1], Harald G. L. Schwefel[5,6], and Luis Enrique García Muñoz[1]

[1] Universidad Carlos III de Madrid, Leganés, Spain, legarcia@ing.uc3m.es

[2] Max Planck Institute for the Science of Light, Erlangen, Germany

[3] SAOT, School in Advanced Optical Technologies, Paul-Gordan-Str. 6, 91052 Erlangen, Germany

[4] Institute of Science and Technology Austria, am Campus 1, 3600 Klosterneuburg, Austria

[5] The Dodd-Walls Centre for Photonic and Quantum Technologies, New Zealand

[6] Department of Physics, University of Otago, Dunedin, New Zealand

***Abstract*— In this paper we present a room temperature radiometer that can eliminate the need of using cryostats in satellite payload reducing its weight and improving reliability. The proposed radiometer is based on an electro-optic upconverter that boosts up microwave photons energy by upconverting them into an optical domain what makes them immune to thermal noise even if operating at room temperature. The converter uses a high-quality factor whispering gallery mode (WGM) resonator providing naturally narrow bandwidth and therefore might be useful for applications like microwave hyperspectral sensing. The upconversion process is explained by providing essential information about photon conversion efficiency and sensitivity. To prove the concept, we describe an experiment which shows state-of-the-art photon conversion efficiency $\eta = 10^{-5}$ per mW of pump power at the frequency of 80 GHz.**

***Index Terms*—radiometry, photonic upconverter, WGM.**

I. INTRODUCTION

Remote sensing is an inherent part of systems focused on data collection for scientific and environmental space observation. Particularly a subject of interest might be a weather forecast and monitoring of climate changes on the Earth. Recently, special attention attracts microwave hyperspectral sensing for vertical profiling of the atmosphere. Currently running meteorological satellites measure vertical distribution of temperature and water vapour in the atmosphere. The 3D temperature profile can be obtained by sampling microwave radiation spectrum at frequencies around oxygen absorption lines. The water vapour profile is measured in similar way around water absorption lines [1]. High spatial resolution and reduced size of radiometers within high available opacity of the atmosphere make natural choice to use mm-wave frequency bands at 60 GHz and 183 GHz for temperature and water vapour profile measurements, respectively. The central point of the radiometry is detection of very weak signals in relation to the noise generated by the receiver itself. It is crucial for measurement sensitivity to minimize receiver internal noise. There is a vast variety of technology that face the problem and can be classified in two divisions related to the operating temperature. Instruments in the first group require cooling down to cryogenic temperatures. That group is represented by TES bolometers [2], SIS mixers [3] and HEMT LNAs [4]. In opposite to them are devices that do not require cryogenic conditions but pay a penalty of significantly higher noise temperature. To the second group belong Schottky diode mixers [5] and HEMT LNAs operating without cooling. Based on sensitivity criteria cryogenic solutions are preferable for satellite earth observation missions. Unfortunately, the cryostat adds significant weight and volume increasing complexity and general cost of launching satellites. Moreover, operational time of the satellite's payload depends on a lifetime of the cryostat [6]. To solve that problem a new type of radiometer operating at room temperature is proposed. An alternative radiometer approach is based on boosting up microwave photon energy by upconverting the signal to the optical domain [7]. The key reason why we are interested in this type of solution is negligible thermal noise in the optical frequency range. It is due to significantly higher energy of the optical photons what makes them immune to relatively weak thermal noise of the receiver even at room temperature. To quantify the phenomenon, we use Planck function to express a ratio of the thermal noise power density to the photon energy [8]

$$\Theta_v(T) = (\exp(hv/k_B T) - 1)^{-1} \quad (1)$$

where h and k_B are Planck and Boltzmann constants respectively. At room temperature (300 K) the ratio is 14 orders of magnitude smaller for the optical domain at 193.54 THz than for microwaves at 200 GHz. The signal is upconverted before thermal noise populates, therefore the detector based on proposed scheme makes it possible to approach the quantum limit of sensitivity when operating at room temperature [9]. Moreover, the solution is easily scalable in frequency in contrast to semiconductor devices, thus operating in mm-wave and submm-wave ranges does not degrade performance of the radiometer.

The paper is organized as follows. In Section 2 we present the electro-optic frequency converter with essential details

required to understand the conversion process (2A) and sensitivity of the proposed radiometer (2B). The experimental set-up showing the state-of-the-art photon conversion efficiency surpassing previous results by two orders of magnitude is presented in Section 3. The conclusions are in Section 4.

II. ELECTRO-OPTIC UPCONVERTER

Electro-optic converters use second order susceptibility $\chi^{(2)}$ of a dielectric material to provide a nonlinear element in a mixing process. The value of $\chi^{(2)}$ is typically a few pm/V [7] what forces using possibly high field intensity to achieve a high photon conversion efficiency η, defined as the ratio of the output and input photon numbers. One of possible solutions is using high power laser pump, but in this case, it is not a practical approach due to limited power supply in satellites and limited heat dissipation of the crystal resonator that may lead to damage. A different approach uses high-Q WGM (Whispering Gallery Modes) resonators to enhance field intensity in a crystal pumped by continuous wave (CW) laser [10]. The unique property of WGMs is that they propagate in a small volume at the rim of the resonator increasing interaction between microwave and optical modes. In result of a three-wave mixing process from the microwave signal at frequency v and laser pump at frequency v_p we obtain two sidebands at frequencies $v_s = v_p \pm v$. The upper and lower sidebands are created due to sum frequency generation (SFG) and difference frequency generation (DFG) processes, respectively [10]. It was shown in [11] that nearly 100% efficiency is theoretically achievable when only SFG is allowed. Moreover, SFG process is preferable to improve noise performance as it is free from spontaneous parametric down conversion noise [12, 13]. Single sideband WGM modulator can be designed by taking advantage of modes degeneration in the resonator that leads to avoided crossing [10]. Basic frequency conversion setup consists of the laser pump working at standard telecom frequency around 193.54 THz (1550 nm) coupled to the WGM resonator via a prism and the microwave signal coupled by a dielectric rod waveguide. Both signals use evanescent field as a coupling mechanism [7]. The upconverted signal can be outcoupled through the same prism. The setup is depicted in Fig. 1.

A. Conversion efficiency and whispering gallery modes

The photon conversion efficiency depends on the resonator geometry and material properties, spatial distribution of WGMs in the resonator, coupling rates and the power of the pump. Moreover, there are two essential conditions to satisfy to achieve high conversion efficiency. The first is straightforward and represents energy conservation of the converter as a quantum-mechanical system

$$hv + hv_s + hv_p = 0. \tag{2}$$

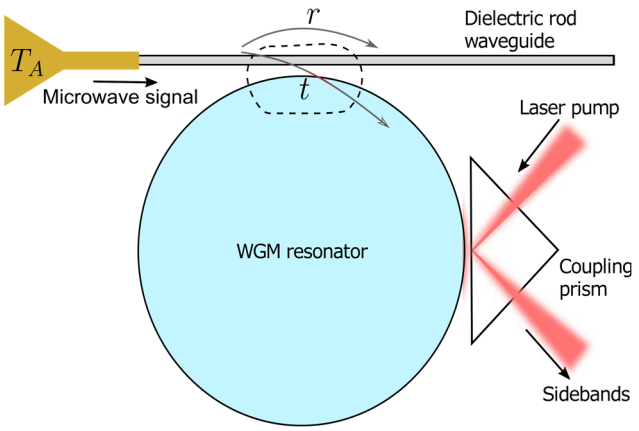

Fig. 1. Electro-optic upconverter based on WGM nonlinear crystal resonator. A microwave and optical modes are coupled to the resonator by an evanescent field of a dielectric waveguide rode and a prism, respectively. The interaction of the modes results in upconverted signal that appears in a form of sidebands which are outcoupled via the prism. A coupling coefficient for the microwave mode is designated as t.

The second refers to the phase-matching that is related to spatial distribution of the modes and will be explained later in this section. Under assumption of critically coupled pump we can express photon conversion efficiency with [10, 14],

$$\eta = P_p Q_p Q_s \frac{g^2}{\pi h v_p^2 v_s} \left(\frac{Q_s}{Q_s^c}\right) \tau F, \tag{3}$$

where P_p is the pump power, Q_p and Q_s are the loaded quality factors of the pump and sideband, respectively, Q_s^c is a coupling quality factor of the sidebands, τ describes roundtrip time in the resonator and F is a power enhancement of the microwave mode understood as the ratio of the intracavity power to the input power. A nonlinear coupling g describes the impact of spatial modes distribution on the conversion efficiency and is given by

$$g = \chi^{(2)} \zeta \frac{\int_V \boldsymbol{\Psi_p} \boldsymbol{\Psi} \boldsymbol{\Psi_s^*}\, dV}{\sqrt{\int_V |\boldsymbol{\Psi_p}|\, dV \int_V |\boldsymbol{\Psi}| dV \int_V |\boldsymbol{\Psi_s}|\, dV}}, \tag{4}$$

where $\zeta = 4\pi\varepsilon_0 \left(\frac{h}{8}\right)^{\frac{1}{2}} (v_p v_s v)^{\frac{1}{2}} / (\varepsilon_p \varepsilon_s \varepsilon)$ with ε_p, ε_s, ε being pump, sideband and microwave permitivities of the media, $\boldsymbol{\Psi_p}$, $\boldsymbol{\Psi}$, $\boldsymbol{\Psi_s}$ are vector eigenfunctions representing field distributions of the pump, microwave and sideband modes. The modes overlap is represented by the integral in the numerator. Integrals in the denominator have meaning of the mode volumes. To the best of our knowledge, field distribution of WGM is found analytically only for resonators with a spherical symmetry, however a good approximation is available in case of a disk-shape resonators for resonances in the optical domain, where the resonator is electrically large [15]. The microwave resonances can be found with aid of full-wave simulators. WGMs are classified due to field distribution inside the resonator and are described by the

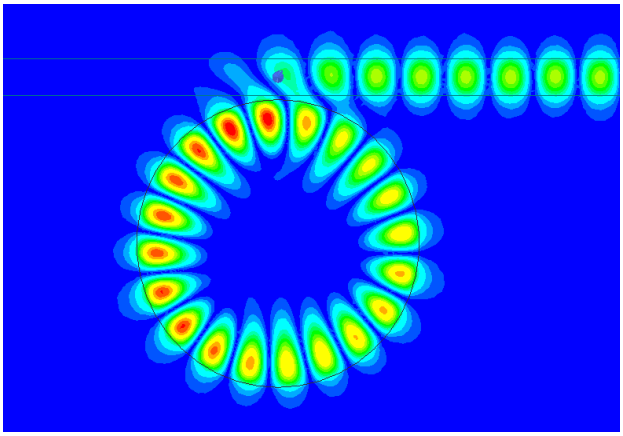

Fig. 2. Example of field distribution of a whispering gallery mode for an azimuthal mode number $m = 10$.

number of zeros in the radial direction q, the number of maxima in the azimuthal direction $\pm m$, where the sign depends on the clockwise or counter clockwise direction of propagation, and the number of maxima in the polar direction $p = m - l + 1$, where l is the polar number [7]. Due to rotational symmetry of the resonator we distinguish azimuthal dependence of the eigenfunction

$$\mathbf{\Psi}(\mathrm{r}, \Theta, \varphi), = \mathbf{\Psi}'(r, \Theta)\mathrm{e}^{\pm im\varphi}. \tag{5}$$

The modes overlap integral takes non-zero value only when angular momenta condition is preserved. The condition is known as phase matching and is given by

$$m_p - m_s = \pm m, \tag{6}$$

where m_p, m_s and m are pump, sideband and microwave signal azimuthal numbers, respectively. It is the only phase matching condition in the most common case $|m| = l$. Modes with higher polar mode order have additional requirements for phase matching that must be taken into account [7]. An example of microwave signal mode in a mm-size disk resonator, obtained from full-wave simulation (HFSS) is depicted in Fig. 2.

B. Sensitivity

Signal power measured by radiometers can be expressed as its equivalent temperature T_A (Rayleigh-Jeans units). The sensitivity of the radiometer is given by a standard deviation of the measured signal power ΔT. Noise performance of the radiometer depends on its thermal noise as well as on photon shot noise described by Mandel's formula [16]. A semi-classical radiometer equation considers both and is given by [17]

$$\Delta T = \frac{T_A + T_e}{\sqrt{\Delta v \Delta t}}\left(1 + \frac{hv}{\eta k_B (T_A + T_e)}\right)^{1/2}, \tag{7}$$

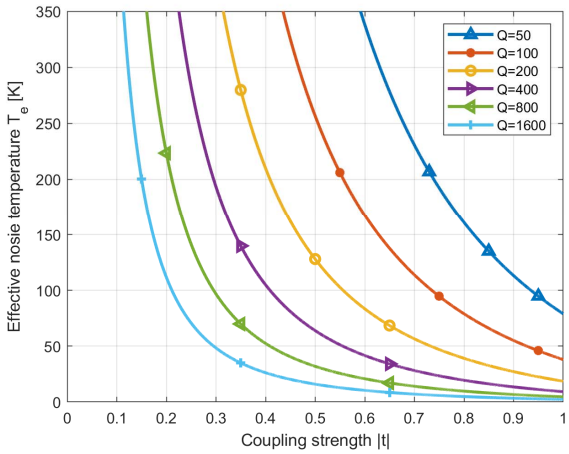

Fig. 3. Effective thermal noise temperature as a function of coupling strength $|t|$ plotted for few values of microwave mode quality factors.

where Δv is bandwidth of the upconverted signal, Δt is integration time and T_e is an effective temperature of the upconverted thermal noise (it is not physical temperature of the resonator). The photon shot noise contribution scales with $\eta^{-1/2}$ and might be significant for low photon conversion efficiency. The semi-classical formula converges to the classical radiometer equation for $hv \ll \mu k_B(T_A + T_e)$. A competitiveness of presented radiometer relies on radiative cooling of WGMs. It was derived in [9] that the effective temperature of the upconverted thermal noise can be significantly lower than the physical temperature of the radiometer when the microwave mode is overcoupled to the resonator. The relation between effective noise temperature and the physical temperature T_{phys} is given by

$$T_e = \left[\frac{(1-a^2(1-|t|^2))\ln(a^{-2})}{(1-a^2)|t|^2} - 1\right] T_{phys}, \tag{8}$$

where, $|t|$ is microwave coupling strength (see Fig. 1) and

$$a^2 = \exp(-2\pi|m|/Q) \tag{9}$$

is roundtrip power attenuation of the mode with Q as its intrinsic quality factor. The effective thermal noise temperature is plotted as a function of coupling strength for physical temperature 300 K in Fig. 3. It was shown in [9, 17] that for high conversion efficiency $\eta = 10^{-2}$, the estimated sensitivity of the proposed radiometer scheme operating at room temperature is comparable or possible better than state-of-the-art cooled mm/submm-wave LNAs.

III. EXPERIMENT

The conducted experiment is focused on optimizing resonator shape to fulfil the phase-matching condition and thus maximize the photon conversion efficiency. Due to manufacturing tolerance limits, phase-matching was optimized by changing iteratively a radius of a disk-shape resonator. The upconversion scheme was tested at 80 GHz using the setup presented in Fig. 4. The central component in the setup is z-cut lithium niobite (LiNbO3) resonator with a diameter of 5.66 mm. The microwave signal is generated by photomixing two telecom lasers relatively detuned by the required frequency, then it is coupled to a dielectric waveguide rod made of gallium arsenide [18] and so on to the resonator. To control the microwave spectrum of the resonator a photomixer receiver is set up. It is synchronized with the emitter to share the same beat frequency. The pump signal is generated by a 1550 nm tuneable laser polarized and filtered by amplified spontaneous emission (ASE) filter. The filter is used to decrease noise generated by the laser around the expected frequency of the sideband. An electro-optic modulator is a part of a Pound-Drever-Hall scheme and eliminates the need of temperature stabilization as it locks the laser to the resonance frequency. The laser is focused by a GRIN lens and coupled to the resonator via a diamond prism. The upconverted signal within an outcoming pump is outcoupled through the same prism, focused with a second GRIN lens, coupled to an optical fibre and guided to an optical spectrum analyser (OSA) to characterize the performance of the system. The exact optical mode numbers in Eq. (6) are difficult to define, thus in practice it is more convenient to use a free spectral range (FSR), defined as the difference of two consecutive resonant frequencies of the optical modes. Thus, we can rewrite the phase-match condition as a single equation given by

$$v = |m| \times FSR. \tag{10}$$

In the experiment, phase-matching is achieved by polishing the resonator iteratively reducing its radius. As a result, both microwave signal resonant frequency v and FSR are slightly changed. The tuning steps are presented in Fig. 5. The intersection point of two lines represents phase-matching. Final measurements of the optical modes show 50 % of coupling efficiency, free spectral range FSR=7.883 GHz and bandwidth of 2.45 MHz what gives the intrinsic quality factor around $Q \approx 1.6 \times 10^8$. The microwave mode is coupled with efficiency 90% and the microwave mode resonance frequency is 78.88 GHz. The mode has an intrinsic quality factor around 400 and a power enhancement $F \approx 6$, when critically coupled. For the SFG process and the power of the pump from the range of 0.03-0.33 mW, the normalized photon conversion efficiency was measured $\eta/P_p = (2.5 \pm 0.2) \times 10^{-5}\, mW^{-1}$. Spectrum of the upconverted signal is measured with OSA and depicted in Fig. 6. The result surpasses by two orders of magnitude so far, the reported conversion efficiencies using WGM resonators at mm-waves [19]. It is also 30 times higher

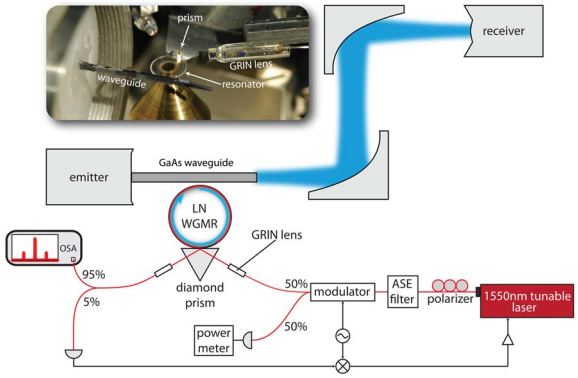

Fig. 4. Setup used in an upconversion experiment.

than state-of-the-art ultra-wideband lithium niobite waveguide phase modulators [20].

IV. CONCLUSIONS

In this paper we presented an alternative radiometer that does not require cooling down to cryogenic temperature. Eliminating the need of using a cryostat makes a payload compact, improves its reliability and therefore it might extend satellite's mission lifetime. The proposed solution can be especially useful for microwave hyperspectral sensing due to requirement of narrow-bandwidth channels. The selectivity is provided by electro-optic upconverter based on nonlinear WGM resonators that are characterized by extremely high-Q of the order of 10^8 at optical frequencies. High sensitivity of the radiometer operating at room temperature is provided by radiative cooling the overcoupled microwave mode. To compete with state-of-the-art LNAs the photon conversion efficiency must be improved from 10^{-5}, measured in the

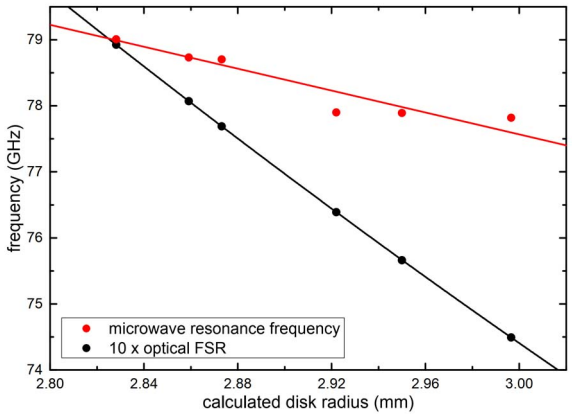

Fig. 5. Visualization of iterative steps in phase matching. The phase matching was achieved by polishing the crystal and reducing its radius. The process increases microwave resonance frequency as well as FSR of the optical mode. A difference in changes rate makes it possible to achieve phase matching at the lines cross point.

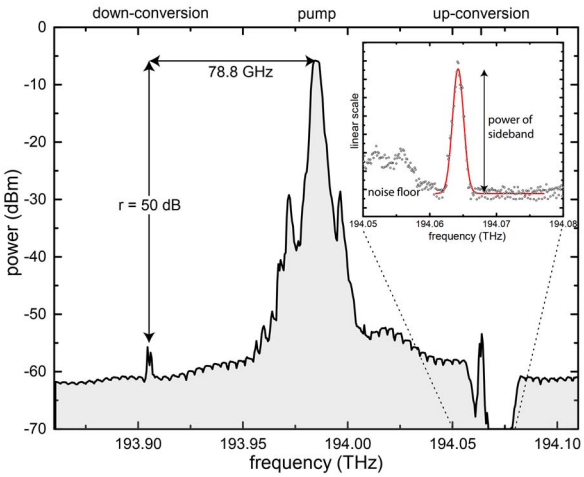

Fig. 6. Spectrum of the pump and upconverted sidebands. The magnified part presents the upper sideband.

experiment to 10^{-2}. The efficiency may be increased by providing better modes overlap [21] and considering materials with higher nonlinearity.

ACKNOWLEDGMENT

This work has been financially supported by Comunidad de Madrid S2018/NMT-4333 MARTINLARA-CM projects, and "FUNDACIÓN SENER" REFTA projects.

REFERENCES

[1] F. Aires et al., "Microwave hyperspectral measurements for temperature and humidity atmospheric profiling from satellite: The clear-sky case." Journal of Geophysical Research: Atmospheres, vol. 120, no. 4, October 2015.

[2] M. J. Myers et al., "Antenna-coupled bolometers for millimeter waves," in IEEE Transactions on Applied Superconductivity, vol. 15, no. 2, pp. 564-566, June 2005.

[3] A. R. Kerr et al., "Development of the ALMA Band-3 and Band-6 Sideband-Separating SIS Mixers," in IEEE Transactions on Terahertz Science and Technology, vol. 4, no. 2, pp. 201-212, March 2014.

[4] W. R. Deal et al., "A 670 GHz Low Noise Amplifier with <10 dB Packaged Noise Figure," in IEEE Microwave and Wireless Components Letters, vol. 26, no. 10, pp. 837-839, October 2016.

[5] E. Schlecht et al., "A unique 520–590 GHz biased subharmonically-pumped Schottky mixer." IEEE Microwave and Wireless Components Letters, vol. 17, no. 12, pp. 879-881, 2007.

[6] M. Linder, N. Rando, A. Peacock, B. Collaudin, "Cryogenics in Space – A review of the missions and technologies," in ESA Bulletin 107, August 2001.

[7] D. V. Strekalov, C. Marquardt, A. B. Matsko, H. G. L. Schwefel, and G. Leuchs, "Nonlinear and quantum optics with whispering gallery resonators," Journal of Optics, vol. 18, no. 12, 123002, 2016.

[8] H. A. Haus, "Thermal noise in dissipative media," Journal of Applied Physics vol. 32, pp. 493-500, 1961.

[9] G. S. Botello et al., "Sensitivity limits of millimeter-wave photonic radiometers based on efficient electro-optic upconverters," Optica, vol. 5, no. 10, pp. 1210-1219, 2018.

[10] A. Rueda et al., "Efficient microwave to optical photon conversion: an electro-optical realization," Optica, vol. 3, pp. 597-604, 2016.

[11] A. B. Matsko, D. V. Strekalov, and N. Yu, "Sensitivity of terahertz photonic receivers," Physical Review A, vol. 77, 043812, 2008.

[12] D. N. Klyshko, "Photons and Nonlinear Optics," CRC Press, 1988.

[13] V. V. Kornienko, G. K. Kitaeva, F. Sedlmeir, G. Leuchs, and H. G. L. Schwefel, "Towards terahertz detection and calibration through spontaneous parametric down-conversion in the terahertz idler-frequency range generated by a 795 nm diode laser system," APL Photonics, vol. 3, 051704, 2018.

[14] D. V. Strekalov et al., "Microwave whispering gallery resonator for efficient optical up-conversion," Physical Review A, vol. 80, 033810, 2009.

[15] I. Breunig, B. Sturman, F. Sedlmeir, H. G. L. Schwefel, and K. Buse, "Whispering gallery modes at the rim of an axisymmetric optical resonator: analytical versus numerical description and comparison with experiment," Optics Express, vol. 21, pp. 30683–30692, 2013.

[16] L. Rodney, "The Quantum Theory of Light," Oxford, 1973.

[17] G. S. Botello, K. A. Abdalmalak, D. Segovia-Vargas, and L. E. Garcia Muñoz, "Photonic upconversion for THz radiometry," in 44th International Conference on Infrared, Millimeter, and Terahertz Waves (IRMMW-THz), Paris, 2019.

[18] A. Rivera-Lavado et al., "Design of a dielectric rod waveguide antenna array for millimeter waves." Journal of Infrared, Millimeter, and Terahertz Waves, vol. 38, no.1, pp. 33-46, 2017.

[19] D. V. Strekalov, A. A. Savchenkov, A. B. Matsko, and N. Yu, "Efficient upconversion of subterahertz radiation in a high-Q whispering gallery resonator," Optics letters, vol. 34, pp. 713–715, 2009.

[20] A. J. Mercante, S. Shi, P. Yao, L. Xie, R. M. Weikle, and D. W. Prather, "Thin film lithium niobate electro-optic modulator with terahertz operating bandwidth," Optica Express, vol. 26, pp. 14810-14816, 2018.

[21] K. A. Abdalmalak et al., "Microwave Radiation Coupling into a WGM Resonator for a High-Photonic-Efficiency Nonlinear Receiver," in 48th European Microwave Conference (EuMC), Madrid, pp. 781-784, 2018.